Chinese Chemical Letters 31 (2020) 249–252

Contents lists available at ScienceDirect

Chinese Chemical Letters

journal homepage: www.elsevier.com/locate/cclet

Communication

A general strategy for one-step fabrication of biocompatible microcapsules with controlled active release

Zeyong Sun[a,1], Chenjing Yang[a,b,1], Max Eggersdorfer[c], Jiecheng Cui[c], Yiwei Li[c], Mingtan Hai[c], Dong Chen[a,b,c,*], David A. Weitz[c,**]

[a] College of Energy Engineering, Zhejiang University, Hangzhou 310027, China
[b] State Key Laboratory of Fluid Power and Mechatronic Systems, Zhejiang University, Hangzhou 310027, China
[c] John A. Paulson School of Engineering and Applied Sciences, Harvard University, Cambridge, MA 02138, United States

ARTICLE INFO

Article history:
Received 10 March 2019
Received in revised form 10 April 2019
Accepted 16 April 2019
Available online 18 April 2019

Keywords:
Microfluidics
Microcapsules
Controlled release
Biocompatible
Single emulsion

ABSTRACT

Fabrication of biocompatible core-shell microcapsules in a controllable and scalable manner remains an important but challenging task. Here, we develop a one-step microfluidic approach for the high-throughput production of biocompatible microcapsules, which utilizes single emulsions as templates and controls the precipitation of biocompatible polymer at the water/oil interface. The facile method enables the loading of various oils in the core and the enhancement of polymer shell strength by polyelectrolyte coating. The resulting microcapsules have the advantages of controllability, scalability, biocompatibility, high encapsulation efficiency and high loading capacity. The core-shell microcapsules are ideal delivery vehicles for programmable active release and various controlled release mechanisms are demonstrated, including burst release by vigorous shaking, pH-triggered release for targeted intestinal release and sustained release of perfume over a long period of time. The utility of our technique paves the way for practical applications of core-shell microcapsules.

Microcapsules with a hierarchical core-shell structure could entrap various actives in the core and control their release; they promise a great potential in a wide variety of applications, including nutrient preservation, fragrance release and drug delivery [1]. The inner core of microcapsules provides an ample space for the loading of various actives, while the outer shell acts as an effective barrier to protect the actives from harsh ambient environments [2,3]. When the shell of microcapsules undergoes a physical or chemical change in response to external stimulus, such as pH, temperature, light, ultrasound or electric field, the cargos are released from the microcapsules [4–9]. To meet the requirements of practical applications, a lot of efforts have been dedicated to the design and high-through fabrication of core-shell microcapsules with programmable release profiles [10–16].

Microcapsules are generally fabricated by bottom-up or top-down methods. In bottom-up approaches, core-shell microcapsules are typically made in two steps: the formation of a single-emulsion core followed by the encapsulation of the single-emulsion core in a shell. The single emulsions are generally prepared by shearing, such as homogenization, which inevitably introduces significant variability in the size. The shell of the microcapsules could be synthesized by secondary emulsification that forms double emulsions, coacervation of positive and negative polymers that deposits a thin layer around the core, or interfacial polymerization that generates a shell at the interface [17]. Therefore, due to the lack of control over the two-step process, core-shell microcapsules produced by the bottom-up approaches are typically characterized by a significant variation in size and property.

With the advent of microfluidics [18], various top-down techniques have been developed for the continuous production of core-shell microcapsules [19,20]. By virtue of its precise control, double emulsions with controlled size and hierarchical structure are directly assembled in microfluidic channels; these double emulsions are generally used as templates to prepared core-shell microcapsules followed by precipitation or cross-linking of polymer in the middle phase [21]. Microcapsules of various shells, such as liposome, colloidosome and polymersome [22,23], have been successfully prepared by the top-down microfluidic

* Corresponding author at: State Key Laboratory of Fluid Power and Mechatronic Systems, Zhejiang University, Hangzhou 310027, China.
** Corresponding author.
E-mail addresses: chen_dong@zju.edu.cn (D. Chen), weitz@seas.harvard.edu (D.A. Weitz).
[1] These authors contribute equally to this work.

https://doi.org/10.1016/j.cclet.2019.04.040
1001-8417/

approaches, showing better control over the size, structure and property than those prepared by conventional bottom-up methods. However, the widespread applications of microcapsules prepared using double emulsions as templates are restricted by the scalability of double emulsions by microfluidics. In addition, toxic organic solvents are generally used to dissolve the polymer in the middle phase, which is problematic for applications in cosmetic, food and drug delivery. Therefore, a high-throughput green preparation of biocompatible microcapsules with controlled structure and property is desired to encapsulate actives and provide a controllable release profile.

Here, we develop a versatile one-step microfluidic approach that uses single emulsion as templates and prepares biocompatible microcapsules via solvent diffusion and polymer precipitation. The obtained core-shell microcapsules harness the advantages of both microcapsules prepared by bottom-up methods, such as easy-to-make and scalable, and microcapsules prepared by top-down methods, such as precise control over the size and shell thickness, high loading capacity and high encapsulation efficiency. We demonstrate the successful encapsulation of various oil actives in the core and show different controlled release mechanisms of the actives from the microcapsules, including burst release, pH-triggered release and sustained release. Our strategy, therefore, provides a general method to prepare biocompatible microcapsules with a programmable release profile, showing a great potential for their practical use in cosmetic, food and drug delivery.

To synthesize the microcapsules, we use shellac, an FDA-approved natural resin mainly consisted of a mixture of polyesters and single esters (Fig. S1 in Supporting information), as our shell material [24]. Shellac polymer barely dissolves in neat oil, while a small amount of ethanol make the oil a decent solvent for shellac, as shown in Fig. S2 (Supporting information). The inner solution of shellac in the ethanol/oil mixture is first emulsified into single droplets using a flow-focusing microfluidic device, as sketched in Fig. 1a. As a result of the competition between interfacial tension, which holds the drop to the tip, and viscous drag, which pulls the drop downstream, monodisperse oil-in-water droplets are generated in the dripping regime, as shown in Fig. 1b. Following droplet formation, ethanol continuously diffuses into the outer aqueous phase, leading to the precipitation of shellac. To minimize the total interfacial energy, shellac precipitates at the periphery of the oil droplets, forming a thin polymer shell that encapsulates oil in the core, as shown in Fig. 1c and modeled in Fig. 1d. Because the solid shell scatters lighter than the oil core, a dark layer around the oil core is observed under optical microscope, as shown in Fig. 1e. When both water and oil are removed, the solidified polymer shell of the resultant microcapsules is visualized by the optical image in Fig. 1f and the SEM image in Fig. 1g.

The versatile method of making biocompatible microcapsules is applicable to various oils, including perfume, lavender oil, rosemary oil, and α-tocopherol, as shown in Figs. 2a–h. Interestingly, for all the four oils, we observe a same tendency that shellac polymer precipitates at the water/oil interface and forms a thin shell at the periphery of the oil core as ethanol diffuses into water. Generally, the precipitation behavior of a polymer upon solvent diffusion is determined by the spreading coefficients [30]. The calculation of the spreading coefficient, $S = \gamma_{oil/water} - (\gamma_{water/shellac} + \gamma_{oil/shellac})$, suggests that the precipitation of shellac at the water/oil interface, which replaces the oil/water interface with the water/shellac and oil/shellac interfaces, lowers the total interfacial energy with $S > 0$, as shown in Table 1. The tendency of shellac polymer to wet both oil and water is attributed to its hydrophobic nature, which leads to a small contact angle with the oil phase, and its carboxyclic groups, which ionize when in contact with water.

The developed one-step microfluidic approach to fabricate biocompatible microcapsules has various advantages, including monodispersity, scalability, controlled microcapsule size, tunable shell thickness, high encapsulation efficiency and high loading capacity. Since the microcapsules are synthesized using single emulsions as templates, they are monodisperse and could simply be scaled up by step-emulsification or membrane emulsification [31]. Their desired size could be achieved by adjusting the flow rates. We obtain monodisperse

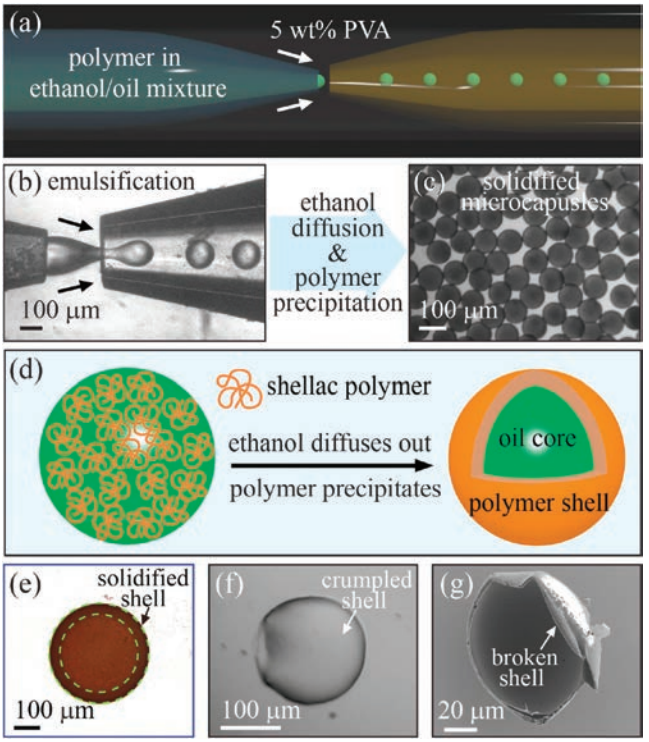

Fig. 1. One-step fabrication of biocompatible microcapsules using single emulsions as templates. (a) Schematic illustration of a flow-focusing glass-capillary microfluidic device. (b) Snapshot of the inner solution of shellac in the ethanol/oil mixture emulsified into monodisperse droplets in the dripping regime. (c) Optical image of monodisperse microcapsules with a solidified shell after solvent diffusion and polymer precipitation. (d) Schematic illustration of the precipitation of shellac polymer at the water/oil interface and the formation of a solid polymer shell as ethanol diffuses into the continuous aqueous phase. (e) The solid shell scatters more light than the oil core, appearing as a dark ring. (f) Optical image of an empty microcapsule after the evaporation of both water and oil. (g) SEM image showing the cross-section of a solid shell.

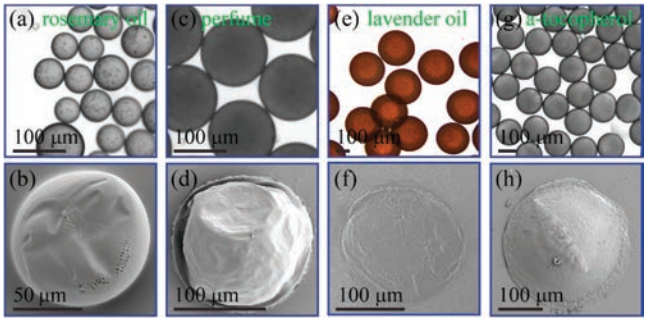

Fig. 2. A universal strategy for the one-step fabrication of biocompatible microcapsules with various oils in the core. Optical and SEM images of microcapsules loaded with (a) and (b) rosemary oil, (c) and (d) perfume, (e) and (f) lavender oil, (g) and (h) α-tocopherol, respectively. All the microcapsules are prepared following the same one-step emulsification process and the different morphologies of the microcapsules are attributed to the different oil viscosities, which influence the polymer precipitation rate.

Table 1
Calculation of the spreading coefficient $S = \gamma_{oil/water} - (\gamma_{water/shellac} + \gamma_{oil/shellac})$. [a]

	Rosemary oil	Perfume	Lavender oil	α-Tocopherol
$\gamma_{oil/water}$ (mN/m)	16.2 [25]	13.18	14.94	16.08
$\theta_{oil/shellac}$	1.57°	2.64°	3.91°	19.21°
$\gamma_{oil/air}$ (mN/m)	29.8 [26]	31.9 [27]	28 [28]	35 [29]
$\gamma_{oil/shellac}$ (mN/m)	6.21	4.13	8.07	2.95
S	3.28	2.34	0.19	6.42

The oil/water interfacial tension is measured by pendent drop experiments. The oil/shellac contact angle is measured by optical microscope. The oil/shellac interfacial tension is calculated using Young's equation and the water/shellac interfacial tension $\gamma_{shellac/water} = 6.71$ mN/m is obtained from the literature [11].

microcapsules with an average size of $d \sim 124$ μm using an inner phase flow rate of $q_i = 100$ μL/h and an outer phase flow rate of $q_o = 1000$ μL/h, as shown in Fig. S3a (Supporting information). When we apply a stronger shear force to the inner phase and increase the outer phase flow rate to $q_o = 2000$ μL/h, we obtain smaller microcapsules with an average size of $d \sim 94$ μm, as shown in Fig. S3b (Supporting information). The microcapsules overall have a very thin shell. For a microcapsule with a diameter of $d \sim 100$ μm prepared using 100 mg/mL shellac in the ethanol/oil mixture (volume ratio of ethanol:oil = 1:4), it only has a shell thickness of $t \sim 1.9$ μm. The shell thickness can be increased by increasing the concentration of shellac in the ethanol/oil mixture or increasing the ethanol ratio. The encapsulation efficiency of the microcapsules is very high, as each individual droplet is turned into a microcapsule. The loading capacity is also very high due to the very thin polymer shell and is 89% for a typical microcapsule with $d \sim 124$ μm and $t \sim 2.4$ μm. Therefore, the versatile one-step microfluidic approach provides a large flexibility to tune the properties of biocompatible microcapsules that could address the demand of practical applications.

Microcapsules prepared by the direct precipitation of shellac polymer at the water/oil interface overall have a low mechanical strength. One simple way to improve the mechanical strength is coating a thin layer of polyelectrolytes on their surface. Shellac microcapsules are negatively charged at neutral pH, due to the partial dissociation of carboxylic groups at the surface, as modeled in Fig. 3a. When negatively charged microcapsules are collected in an aqueous solution with 0.5 wt% chitosan, which is positively charged due to its amine groups, chitosan electrostatically binds to the surface of the microcapsules, as modeled in Fig. 3b. Without polyelectrolyte coating, most of the microcapsules break when the sample is dried, as shown in Figs. S4a and b (Supporting information), and their shells show a very low integrity, as shown in Fig. 3c and magnified in Fig. 3d. In contrast, when coated with positive polyelectrolytes, the microcapsules exhibit a remarkable better mechanical strength, evidenced by the fact that most of the microcapsules retain their spherical shape when the sample is dried, as shown in Figs. S4c and d (Supporting information). The shells of polyelectrolyte-coated microcapsules also show a very dense texture, as characterized by the SEM images in Figs. 3e and f. Therefore, the complexation of negatively charged microcapsules with positively charged chitosan polymer *via* electrostatic interaction could greatly improve the mechanical strength of the microcapsules.

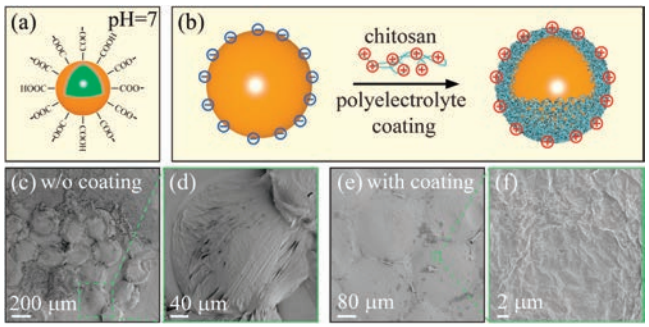

Fig. 3. Enhancement of the mechanical strength of the microcapsules by polyelectrolyte coating. (a) Shellac microcapsules are negatively charged at neutral pH, due to the partial dissociation of carboxylic groups at the surface. (b) Schematic illustration of polyelectrolyte coating, showing the electrostatic binding of positively charged chitosan to a negatively charged microcapsule. (c) SEM and (d) magnified images of empty microcapsules without polyelectrolyte coating, showing a very low integrity. (e) SEM and (f) magnified images of polyelectrolyte-coated microcapsules. The consolidated shells show a much better integrity and a very dense texture. The oil cores of the microcapsules are removed by ethyl acetate, which barely dissolves shellac.

The microcapsules are ideal carriers for various oil actives and posses excellent diversity for stimuli-triggered release of the cargo. For example, a burst release of oil actives from the microcapsules can be triggered by vigorous shaking, which directly breaks the shell and instantly drives the cargo out off the microcapsules, as shown in Fig. 4a. The microcapsules can also be designed to achieve targeted intestinal release, which is triggered by a pH change in the intestine that dissolves the polymer shell, as modeled in Fig. 4b. To demonstrate the pH-triggered release, we use NaOH as the stimulus and trigger the release of the encapsulated cargo. In the presence of NaOH, most of the carboxylic groups are ionized and the shell of shellac polymer eventually dissolves over a couple of hours, leading to the release of the cargo from the microcapsule, as shown in Figs. 4c–h. Since it is acidic in the stomach and alkaline in the intestine, the microcapsules are useful delivery vehicles for targeted intestinal release. The shell of the microcapsules could protect the drug from the hash environments of the stomach, which may degrade easily or lost activity when exposed to the acidic condition, and prevent the release of the drug in the stomach, which may be harmful to the stomach. The drug is then released in the intestine, when the shells are dissolved under the alkaline condition.

Instead of breaking the microcapsules, the shell could also act as an effective barrier to control the release of cargos over time and tuning the shell thickness provides a simple and effective way to achieve temporal variation of the release kinetics, as modeled in Figs. 5a–c. To demonstrate the sustained release profile, we use lavender oil, a volatile oil, as our model oil active. By simply adjusting the concentration of shellac polymer in the ethanol/oil mixture, we obtain microcapsules with different shell thicknesses and different release profiles of lavender oil from the microcapsules, as shown in Fig. 5d. Without encapsulation, 35% lavender oil evaporates within 2 h and all of them are expected to evaporate within 6 h. When encapsulated in shellac microcapsules with a shell thickness of $t \sim 6.7$ μm, only 20% lavender oil evaporates within 2 h. Further increase of the shell thickness to $t \sim 9.0$ μm extends the whole release period to 16 h. These results suggest that in addition to stimuli-triggered release, shell thickness provides yet another simple means to control the profile of sustained release. Therefore, the diverse release modes of our microcapsules allow the customization of cargo release kinetics for a variety of practical applications.

We develop a versatile one-step single-emulsion-based microfluidic approach to prepare biocompatible core-shell microcapsules and encapsulate a diverse set of oil actives in the core. The solution of shellac polymer in the ethanol/oil mixture is first emulsified in a microfluidic device. Upon ethanol diffusion, shellac polymer precipitates at the water/oil interface, forming a solid thin shell. The obtained thin-shell microcapsules combine the advantages of both microcapsules prepared by top-down and bottom-up methods, showing excellent monodispersity, scalability, controlled microcapsule size, tunable shell

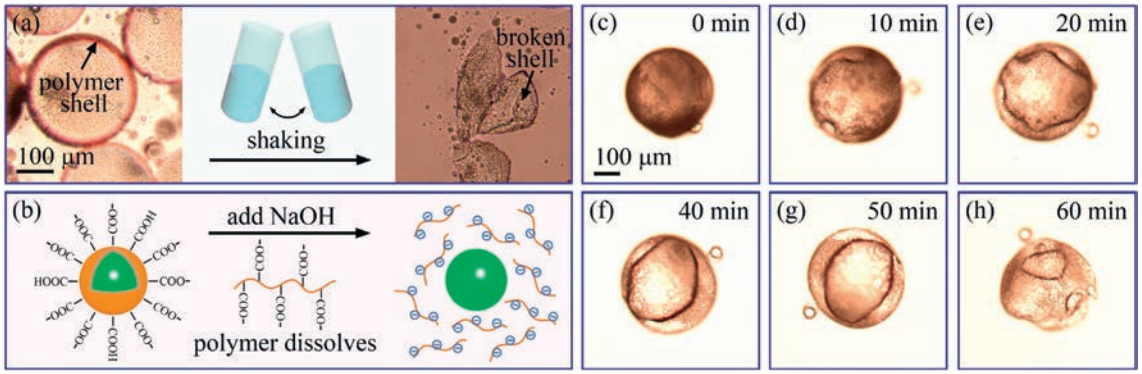

Fig. 4. Burst release and pH-triggered release of shellac microcapsules. (a) Burst release of oils from the microcapsules is triggered by vigorous shaking, showing broken and empty shells. (b) Schematic illustration of pH-triggered release through the dissolution of polymer shell under an alkaline condition. The high dissociation rate of carboxylic groups at alkaline pH makes shellac polymer dissolvable in water. (c–h) Time-lapse optical images, showing the dissolution of a microcapsule after the addition of NaOH.

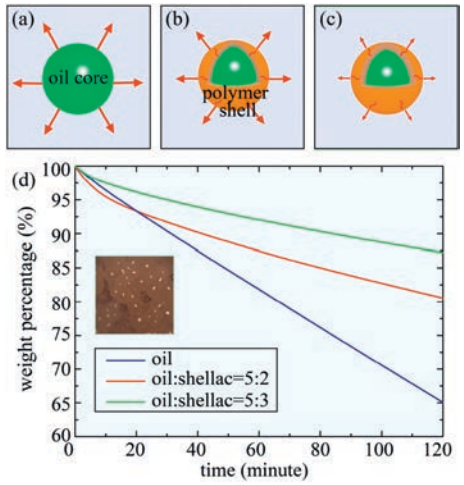

Fig. 5. Sustained release of lavender oil encapsulated in shellac microcapsules. (a) Direct evaporation of lavender oil into air. (b, c) The polymer shell acts as an effective barrier to control the evaporation of lavender oil. The evaporation rate decreases when the polymer shell becomes thicker. (d) Weight percentage of lavender oil encapsulated in microcapsules of different shell thicknesses over time. Without encapsulation, all lavender oil evaporates within 6 h. When encapsulated in shellac microcapsules of $t \sim 6.7$ μm and $t \sim 9.0$ μm, the release profiles of lavender oil are extended to 10 h and 16 h, respectively. Because microcapsules have larger surface area and some microcapsules may break during handling, leaving some oil near the surface, the release rate of oil from the microcapsules is faster at the beginning.

thickness, high encapsulation efficiency and high loading capacity. The microcapsules are excellent delivery vehicles of various oil actives and allow the customization of the cargo release profiles for targeted applications, such as burst release, pH-triggered release and sustained release, thus representing an important step towards their practical applications in cosmetic, food and drug delivery.

Acknowledgments

This work is supported by the National Natural Science Foundation of China (Nos. 21878258 and 11704331), "the Fundamental Research Funds for the Central Universities" (No. 2018QNA4046) and the Youth Funds of the State Key Laboratory of Fluid Power and Mechatronic Systems (Zhejiang University). This work was also supported by the National Science Foundation (No. DMR-1310266) and the Harvard Materials Research Science and Engineering Center (No. DMR-1420570).

Appendix A. Supplementary data

Supplementary material related to this article can be found, in the online version, at doi:https://doi.org/10.1016/j.cclet.2019.04.040.

References

[1] J. Xu, J. Li, Y. Yang, et al., Angew. Chem. 128 (2016) 14853–14857.
[2] E. Amstad, ACS Macro Lett. 6 (2017) 841–847.
[3] X.P. Zhang, J. Luo, D.X. Zhang, et al., J. Colloid Interface Sci. 517 (2018) 86–92.
[4] A.P. Esserkahn, S.A. Odom, N.R. Sottos, et al., Macromolecules 44 (2015) 5539–5553.
[5] J.M. Grolman, B. Inci, J.S. Moore, ACS Macro Lett. 4 (2015) 441–445.
[6] Y. Jia, Y. Ren, L. Hou, et al., Lab Chip 18 (2018) 1121.
[7] X. Liu, P. Zhou, Y. Huang, et al., Angew. Chem. 55 (2016) 7095–7100.
[8] W. Xu, P.A. Ledin, Z. Iatridi, et al., Angew. Chem. Int. Ed. 55 (2016) 4908–4913.
[9] S. Kennedy, J. Hu, C. Kearney, et al., Biomaterials 75 (2016) 91.
[10] H. Zhang, Y. Zhu, L. Qu, et al., Nano Lett. 18 (2018) 1448–1453.
[11] L. Kong, E. Amstad, M. Hai, et al., Chin. Chem. Lett. 28 (2017) 1897–1900.
[12] S. Lee, T.Y. Lee, E. Amstad, S.H. Kim, J. Adv. Mater. Technol. 3 (2018) 1800006.
[13] D. Liu, H. Zhang, S. Cito, et al., Nano Lett. 17 (2017) 606–614.
[14] X.R. You, X.J. Ju, F. He, et al., ACS Appl. Mater. Interfaces 9 (2017) 19258–19268.
[15] F.N. Sang, Z. Chen, Y.D. Wang, J.H. Xu, AIChE J. 64 (2018) 730-739.
[16] W. Deng, H.C. Guo, G.A. Li, C.Y. Kan, Chin. Chem. Lett. 28 (2017) 367–371.
[17] F. Lu, Y. Luo, B. Li, Macromol. Rapid Commun. 28 (2010) 868–874.
[18] C. Liu, W. Zheng, R. Xie, et al., Chin. Chem. Lett. 30 (2019) 457–460.
[19] R. Ran, Q. Sun, T. Baby, et al., Chem. Eng. Sci. 169 (2017) 78–96.
[20] T.Y. Lee, T.M. Choi, T.S. Shim, et al., Lab Chip 16 (2016) 3415–3440.
[21] B.F.B. Silva, C. Rodríguez-Abreu, N. Vilanova, Curr. Opin. Colloid Interface Sci. 25 (2016) 98–108.
[22] S. Zhou, F. Jing, S.S. Datta, et al., Adv. Funct. Mater. 23 (2013) 5925–5929.
[23] C.L. Mou, W. Wang, Z.L. Li, et al., Adv. Sci. 5 (2018) 1700960.
[24] D. Chen, E. Amstad, C.X. Zhao, et al., ACS Nano 11 (2017) 11978–11985.
[25] S. Rodríguez-Rojo, S. Varona, M. Núñez, M.J. Cocero, Ind. Crops Prod. 37 (2012) 137–140.
[26] J.H. Tak, M.B. Isman, Sci. Rep. 5 (2015) 12690.
[27] Y.W. Sheu, C.H. Tu, J. Chem. Eng. Data 50 (2005) 1706–1710.
[28] G. Fenyvesi, R.H. Poladi, H.B. Sunkara, U.S. Patent, US8486458B2, 2013.
[29] S.W. Hwang, K.S. Jin, S.E. Selke, et al., Polym. Int. 61 (2012) 418–425.
[30] A. Loxley, B. Vincent, J. Colloid Interface Sci. 208 (1998) 49–62.
[31] E. Amstad, M. Chemama, M. Eggersdorfer, et al., Lab Chip 16 (2016) 4163.